Journal of Analytical and Applied Pyrolysis 160 (2021) 105359

Contents lists available at ScienceDirect

Journal of Analytical and Applied Pyrolysis

journal homepage: www.elsevier.com/locate/jaap

An insight into the role of biomass, biocompounds and synthetic polymers as additives to coal for the synthesis of carbon foams

E. Rodríguez *, M.A. Diez, C. Antuña-Nieto, M.A. López-Antón, R. García, M. R. Martínez-Tarazona

Instituto de Ciencia y Tecnología del Carbono, INCAR-CSIC, C/ Francisco Pintado Fe, 26, 33011, Oviedo, Spain

ARTICLE INFO

Keywords:
Carbon foam
Thermogravimetry
Fluidity
Co-pyrolysis
Porosity
Thermal conductivity

ABSTRACT

Carbon foams were synthesized from blends of coal and several C-containing additives of different nature, with the aim to study their influence on the foaming step, and hence in the final properties of the obtained foams. The additives included biomass and agricultural products, and thermoplastic and thermosetting polymers, at different concentrations, ranging from 5 to 20 wt%. The effects of the additives on pore structure, carbon matrix and thermal properties of the resulting foams were investigated. The presence of additives during pyrolysis had no effect on the yield of carbonaceous product. However, all the additives, except the polybutadiene phenyl terminated (PBP) elastomer, led to a reduction in the fluidity of the blend. This difference in the effect can be related to the liquid nature of PBP, which favors the impregnation of coal particles, to the decomposition pattern overlapping with that of the coal, and to a high chemical affinity of the degradation products of PBP and coal. Analysis of the fluidity development of the blends and the changes in volatile matter production at different temperature intervals showed that bio-type additives with the maximum emission of volatiles in the coal pre-plastic stage provided improvements in the porosity of the C-foams. In contrast, synthetic polymers like low-density polyethylene (LDPE) and PBP generated most of their thermal degradation products during the plastic and the own thermal degradation stages of coal, leading to a reduction in the porosity of the carbon foams. This behavior can be attributed to a blocking of some macropores in the C-foams by deposition, in the pore mouths, of molten LDPE and/or oligomers from its backbone promoted by the conditions applied during the long residence time inside the reactor. The addition of polyethylene terephthalate (PET) resulted in no foam formation. Regardless of the additive, the resulting foams derived from binary blends showed lower thermal conductivity compared to that synthesized from the unmixed coal. The values of thermal conductivity are closely related to the porous and carbon structure displayed by the foams.

1. Introduction

Carbon foams are 3D-materials with an interconnected open cell structure that are considered excellent structural engineering materials, due to their lightness combined with custom thermal and electrical characteristics. The properties of carbon foams are determined by their structural parameters, such as density, pore size, wall thickness and graphitization degree, among others [1]. The selection of the raw material used as precursor and the synthesis method play an important role in their final application [2–4].

Vitreous carbon foams derived from non-graphitizable precursors, such as synthetic polymers or natural products display low thermal conductivity (<0.5 W m^{-1} K^{-1}), and therefore may be used as thermal protection materials [5–8]. On the other hand, carbon foams produced from such precursors as coal, coal-tar pitch or mesophase pitch present thermal properties that can be tailored based on the thermal history of the raw material. Thus, at about 350–400 °C certain coals and pitches behave like a thermoplastic material, which becomes thermosetting at around 450–500 °C [9]. As a consequence, graphitic foams derived from pitches reach values of thermal conductivity ranging from 100 to 200 W m^{-1} K^{-1} and work well as thermal enhancers [10–12], whereas their carbonized counterparts present lower values, ranging from 0.25 to 4.0 W m^{-1} K^{-1} [10,13]. Specifically, coal-based carbon foams are actually commercialized by Touchstone Research Laboratory, Ltd. (CFOAM®), having competitive prices and properties in applications such as composite core, fire and thermal protection, electromagnetic shielding and

* Corresponding author.
E-mail address: elena@incar.csic.es (E. Rodríguez).

https://doi.org/10.1016/j.jaap.2021.105359
Received 6 September 2021; Received in revised form 11 October 2021; Accepted 23 October 2021
Available online 14 November 2021

radar absorption [13,14].

Coal-based carbon foams are generally synthesized by a self-bubbling method in a pressurized reactor (under inert atmosphere with controlled heating and pressure), followed by carbonization [15,16]. During the foaming process, the coal melts and begins to release volatile matter. These gases create bubbles in the viscous medium that impinge on each other and fracture the melting matter, creating the cell network of the foam. At the same time, the decomposition of the coal causes polymerization and increases viscosity, thus hindering the flow of bubbles and their coalescence. Therefore, the primary porous structure of coal-based foams is conformed during this foaming step and will depend on both the experimental conditions (temperature, pressure) and the rheological characteristics of the coal precursor, such as fluidity and volatile matter content, among others. Subsequently, a carbonization step is carried out to remove the remaining volatile matter and improve mechanical strength.

Foam properties may be also tailored by adding external substances. Thus, several works based on the addition of carbon or mineral fillers to pitch precursors have been carried in order to improve mechanical, electrical and thermal properties [17–19]. However, fewer studies have been attempted to improve coal-based carbon foam properties by blending the foam precursor with additives. Boron compounds were successfully employed to increase their graphitic structure [20–22], whereas chemical activating agents such as KOH or $ZnCl_2$ promote microporosity development [23,24].

Nowadays, many efforts are directed to the development of more eco-friendly technologies based on renewable resources and recycled materials [8]. In this scenario, the co-carbonization of coal blends with other carbon sources derived from agriculture and urban wastes, such as plastics, tires, biomass, etc. has been evaluated as suitable for metallurgical coke production [25–27]. However, until now, these blends have not been studied for carbon foam production.

The aim of the present work is to synthesize coal-based carbon foams using additives of different origin, composition, and chemical structure. Given the importance of the plastic stage during foaming, the interaction of the reactive additives with coal during pyrolysis was evaluated, in order to assess their effect on the final properties of the carbonized foams, such as density, porosity and thermal properties.

2. Materials and methods

2.1. Precursors

Carbon foams were prepared using a high-medium volatile and medium-fluid bituminous coal (TC) as carbon precursor (volatile matter: 31 wt% db, ash: 9.2 wt% db). Coal-based blends were prepared by adding a series of seven organic additives that cover a broad spectrum in origin, chemical composition and structure, and thermal behaviour. They comprise two main groups: synthetic and natural polymers. Within the group of synthetic polymer, sub-classifications can be made based on their behavior during thermal processing (i.e., thermoplastics and thermosets) or the chemical structure of their backbone (C-C, C-O, single or double bonds). Two of the selected synthetic polymers were thermoplastics contained in household wastes: low-density polyethylene (LDPE) and polyethylene terephthalate (PET). The third synthetic polymer was an elastomer, or synthetic rubber, derived from polybutadiene, which is employed in the tire industry: polybutadiene phenyl terminated (PBP), with an average Mn of ~1500, 80% unsaturation, and a composition of 45% trans-1,4, 25% cis-1,4% and 25% vinyl (Aldrich). The organic additives were different kinds of biodegradable polymers of natural origin: (i) pine sawdust (SP), a lignocellulosic biomass derived from the processing, manufacturing industry; two biocompounds that are present in many plants, (ii) tannins (TA) (Agrovin, >68% phenols), mainly consisting of water-soluble polyphenols, and (iii) D(+)-sucrose (SU) (Carlo Erba, ACS grade +99%), a disaccharide consisting of two monosaccharides, glucose and fructose; and (iv) orange peel (OP), an agricultural biowaste rich in pectin, cellulose, and hemicellulose, which is the main by-product of the citrus processing industry.

Elemental analysis of the raw materials was carried out using a LECO CHN-2000 for C, H and N, and a LECO VTF-900 for the direct determination of oxygen.

2.2. Fluidity development of coal and its blends

The thermoplastic or fluidity properties of the coal and its blends containing 5 or 10% of each additive were assessed by means of a constant-torque Gieseler R.B. Automazione PL2000 plastometer, following the ASTM D2639-74 standard procedure. Briefly, packed samples (5 g, <425 μm) were heated from 340 °C up to nearly 500 °C at a heating rate of 3 °C min^{-1}. The rate at which the stirrer rotates is directly proportional to fluidity and the maximum value reached in dial divisions per minute (ddpm) is taken as the maximum fluidity (Fmax) of the sample at a specific temperature (Tf). The temperatures of initial softening (Ts) and resolidification (Tr) were also recorded and the difference between them is taken to be the fluid or plastic range (PR).

2.3. TGA experiments

The thermogravimetric analysis of the raw materials and binary blends was performed in a thermogravimetric analyzer (TGA/DSC1 Star System Mettler Toledo). Samples were heated from ambient temperature up to 1000 °C at 10 °C min^{-1} under nitrogen atmosphere, at a flow rate of 75 ml min^{-1}. The amounts of volatile matter released up to a specific temperature (VMT), and at specific temperature intervals (VMTx-Ty) were deduced from the weight loss. The temperature of maximum volatile matter released (Tmax) and the maximum rate (DTGmax) were determined from the derivative of weight loss (DTG) curves.

2.4. Synthesis of the carbon foams

The coal-based foams were synthesized following a two-stage procedure: (i) a foaming step, consisting of a pressurized carbonization at a temperature close to that which leads to maximum coal fluidity, and (ii) carbonization under inert atmosphere at 1100 °C [22,28]. Each of the raw materials was ground below 212 μm before use. In a typical experiment, 15 g of coal were physically mixed with the additive (5, 10 or 20 wt%) to generate a homogeneous blend. Then, the mixture was molded and pressed to produce a cylindrical piece, which was loaded into the reactor. The reactor was purged with Ar to provide an inert atmosphere (Pi, 1 bar) and then heated in a fluidized sand bed oven, with a heating rate of 2 °C min-1, up to 465 °C, and a soaking time of 2 h. The outlet valve is kept close during the thermal treatment, so that the volatiles remain in the reactor. The final pressure reached during the foaming process ranged from 15 to 100 bar. The reactor was purged with Ar and then heated in a fluidized sand bed oven, with a heating rate of 2 °C min^{-1}, up to 465 °C, and a soaking time of 2 h. Finally, the resulting "green" foam was heated under inert atmosphere (Ar, 100 ml min^{-1}) at 1100 °C for 2 h, with a heating rate of 1 °C min^{-1}. The carbon foams obtained were denoted as CF*xy*, where *x* refers to the percentage of the additive (from 5 to 20 wt%) and *y* to the type of additive (LDPE, PET, PBP, SP, TA, SU, OP) (see Section 2.1 for details). For comparison purposes, an appropriate, additive-free carbon foam was also prepared and designated as CF.

2.5. Characterization of carbon foams

The chemical composition of the carbon foams was determined by elemental analysis as described in Section 2.1. The skeletal or true density (ρ_{He}) of the carbon foams was measured by means of helium pycnometry, in a Micrometics Accupyc 1330 Pycnometer. The apparent density (ρ_{Hg}), also known as bulk density, was determined with mercury

at 0.005 MPa, in a Micrometics Autopore IV 9500 mercury porosimeter. The percentage of open porosity (Ɛ) and the total pore volume (V_{tp}) were calculated from the values of true and apparent densities, as described in reference [21]. Before the analysis, the samples were outgassed at 180 °C overnight.

The morphology of the foams was evaluated by scanning electron microscopy (SEM), using a Zeiss microscope (model DSM 942).

The Raman spectra of the carbon foams obtained at 1100 °C were performed on a Renishaw InVia Qontor spectroscope, equipped with a detector CCD Renishaw Centrus and a laser DPSS (532 nm). A Leica DM2700 microscope with 100x objective lens was used to focus the laser beam. Each first-order Raman spectrum for the carbon foam was deconvoluted to obtain four main components at 1595 (G band), 1520, 1345 (D band) and around 1200 cm^{-1} [29]. The D/G ratio was used as a measure of the degree of structural order in the carbon matrix of the foams.

Thermal conductivity (*k)* was determined by an indirect method using the following equation:

$$k = \alpha \cdot \rho \cdot C_P$$

where *k* is the thermal conductivity (W m^{-1} K^{-1}), α is the thermal diffusivity (mm^2 s^{-1}), C_P is the specific heat (J g^{-1} K^{-1}), and ρ is the apparent density (g cm^{-3}). Thermal diffusivity (α) tests were carried out at 25 °C over samples in disk-like shape, with 12.7 mm diameter and 2.5 mm thickness, by using a NETZSCH/LFA 457 MicroFlash thermal diffusivity analyzer. The specific heat capacity was measured at ambient temperature in a C80 Setaram calorimeter, using Calisto software for data processing.

3. Results and discussion

3.1. Effect of the additives on the fluidity development

Most of the selected organic additives have a significant oxygen content compared to coal. The exceptions are the polyolefin LDPE and the elastomer PBP, which do not incorporate oxygen in their backbone structure (Table 1). It is well known that the presence of heteroatoms in the reaction media leads to a reduction in the plastic properties of coal [26,30]. Therefore, it is expected that such additives will cause changes in thermoplasticity during foaming to different extents, depending on their composition.

The main thermoplastic parameters of coal TC and its binary blends with 5 and 10 w% additive are given in Table 2. In all the coal-additive blends, a loss in Gieseler Fmax occurs, with the extent of the reduction depending on the kind and the amount of the additive. The exceptions are the blends containing the PBP elastomer, which enhances in a large extent this parameter, reaching values 10 times higher than that of the unblended coal. To further study the fluidity increase caused by PBP, blends containing 5 wt% of two commercial polybutadiene-based polymers were also tested: polybutadiene with predominantly 1,2-addition (PB12) (Aldrich, ~90% of 1,2-vinyl) and polybutadiene with predominantly 1,4-addition in *cis* configuration (PBcis) (Aldrich, 98% of cis and average MW of 200.000–300.000). These polymers also produced an increase in the Gieseler Fmax of the blends, the highest being when the PB12 is added (11300 and 7378 ddpm for PB12 and PBcis, respectively). Although PBP and PB12 are the strongest enhancers of fluidity, the fluid temperature range decreases and then, the system is kept in a fluid stage for a shorter time. The Ts of the coal-PBP blend shifts to values 15–19 °C higher than that the unblended coal, while that of the coal-PB12 blend shifts up 27 °C. No significant variation is observed for the coal-PBcis blend.

Table 1
Elemental analysis of the coal and additives (wt% ash free).

	TC	LDPE	PET	PBP	SP	TA	SU	OP
C	86.04	85.72	62.50	88.95	49.83	50.59	42.11	45.76
H	5.37	14.28	4.17	11.05	6.05	4.20	6.43	6.16
N	1.70	0.00	0.00	0.00	0.12	0.00	0.00	0.95
O	6.89	0.00	33.33	0.00	44.00	45.20	51.46	47.13
O/C	0.06	0.00	0.40	0.00	0.66	0.67	0.92	0.77
H/C	0.75	1.99	0.80	1.49	1.46	1.00	1.83	1.62

A different effect can be observed in coal-PET blends. This polymer is the strongest inhibitor of coal fluidity since the fluidity of the blend with 5 wt% addition drastically drops to values as extremely low as 3 ddpm (only 0.1% of the initial fluidity of coal TC), and at 10 wt% the fluidity of the blend is destroyed. A similar behavior can also be observed for the blend with 10 wt% of sucrose. In general, the following order of decreasing coal plasticity can be established:

Additive (wt%)	Higher inhibitor ——→ Lower inhibitor Enhancer
5	PET >> SU > SP > TA > LDPE > OP ——— PBP
10	PET=SU >SP >> OP > TA ≈ LDPE ——— PBP

Based on their plastic range, the additives can be divided into three categories (Table 2): (i) PET, PBP, SU and TA produce a decrease in the temperature fluid interval, due to the higher softening temperature of the blends, being more marked as the concentration is increased; (ii) SP and OP, which do not produce changes in the plastic range, and (iii) LDPE, which slightly increases the plastic range, this effect being more marked as its concentration is increased.

For bio-additives, no clear relation between the oxygen content and the fluidity parameters can be inferred. For example, 5 wt% OP addition produces the lower reduction of fluidity parameters in comparison with the other additives, despite its higher oxygen content. It appears, therefore, that the type of oxygen functionalities, rather than simply oxygen concentration, is the more critical factor in the development of coal fluidity. When comparing the bio-additives (SP, TA and SU), the carbohydrate proportion in the additive could explain the different suppression of fluidity, which agrees with the suppression fluidity order of lignocellulosic wood components: cellulose > lignin > xylan [26].

3.2. Thermal behavior of raw materials

To understand what happens during the plastic stage of the coal and the blends, and to gain further understanding of the influence of additives on coal fluidity development, thermogravimetric analysis was carried out. Bearing in mind that the majority of coking coals become fluid in a temperature range of around 400–500 °C and reach maximum fluidity near 450 °C, the temperature intervals chosen to evaluate the distribution of volatile products in gaseous form of the additives were related to the pre-plastic stage of the coal (up to 400 °C), the plastic or fluid stage of the coal between softening and maximum fluidity in the system (400–450 °C), between the maximum fluidity and resolidification (450–500 °C), and the post-plastic stages (500–750 and 750–1000 °C). The percentage of volatile matter (VM) released by the coal and additives during pyrolysis at these specific temperature intervals are displayed in Fig. 1 and Table S1. The carbon yield at 1000 °C (CY) and the temperature and rate at which the maximum release of VM takes place (T_{max} and DTG_{max}) are also provided in the Supplementary information (see Table S1).

The first point to note in Fig. 1 is that the decomposition of the additives into gaseous products and their release takes place in different quantities and at stages different from the key stage of coal transformation into carbon foams. Fig. 2 shows the DTG curves of the synthetic polymers and the coal. LDPE and PET undergo decomposition in a narrow temperature range (400–500 °C). The degradation products from LDPE are concentrated in the 450–500 °C range, with a Tmax of 477 °C and a DTGmax of 28.03% min^{-1}, whereas PET released the

Table 2
Thermoplastic parameters of the coal TC and its blends with the several additives.

	Additive (%)	Fmax (ddpm)	Ts (°C)	Tf (°C)	Tr (°C)	PR (°C)	Fluidity variation (%)	Residual Fluidity (%)
TC	0	2913	397	442	478	81	0	100
TC5LDPE	5	1550	395	445	479	84	-47	53
TC10LDPE	10	1440	384	444	483	99	-51	49
TC5PET	5	2.6	436	448	478	42	-100	0
TC10PET	10	0	n.d.	n.d.	n.d.	0	-100	0
TC5PBP	5	15719	412	445	484	72	440	540
TC10PBP	10	27762	416	449	485	69	853	953
TC5SP	5	778	397	442	478	81	-73	27
TC10SP	10	133	395	443	476	81	-95	5
TC5TA	5	1126	409	442	477	68	-61	39
TC10TA	10	1346	414	438	477	63	-54	46
TC5SU	5	664	419	446	482	63	-77	23
TC10SU	10	0	n.d.	n.d.	n.d.	0	-100	0
TC5OP	5	2131	399	444	480	81	-27	73
TC10OP	10	1032	399	444	479	80	-65	35

n.d.: no detected; Fmax: maximum fluidity; Ts: initial softening temperature; Tf: temperature of maximum fluidity; Tr: solidification temperature

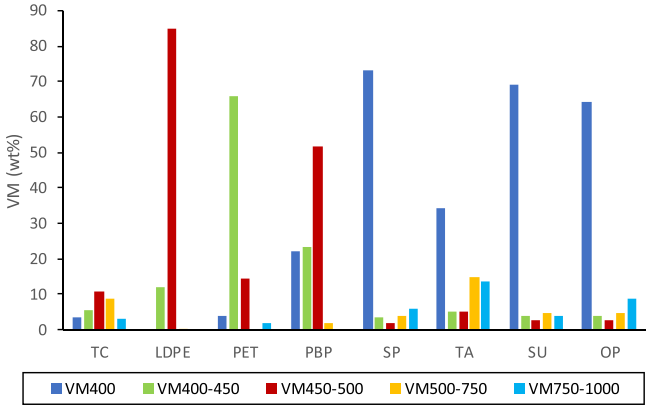

Fig. 1. VM released by the coal and the C-containing additives during pyrolysis at specific temperature ranges.

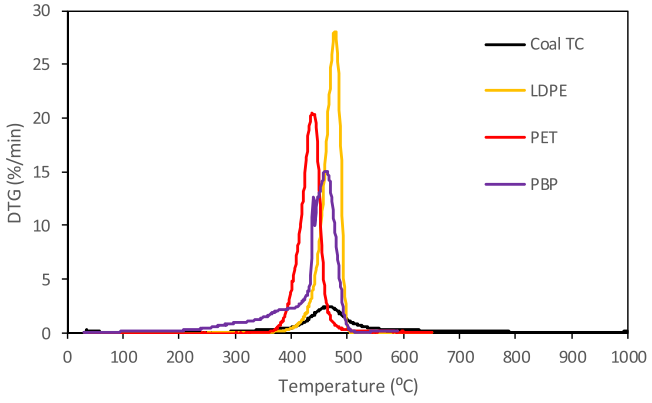

Fig. 2. Comparison of DTG curves corresponding to the synthetic polymers and the coal.

largest quantity at a much lower temperature interval (400–450 °C), with a Tmax of 434 °C and a DTGmax of 20.48% min^{-1} (Table S1). PBP, however, generates about half of the decomposition products in the temperature interval that ranges from 450 to 500 °C, with a contribution of 25% to the other low-temperature stages. The generation of volatile products in the case of synthetic polymers (LDPE, PET and PBP) overlaps with the starting of VM release from the coal, when it starts to soften and becomes fluid. The coal shows a maximum VM evolution at 467 °C, eight times lower than those of the polymers (2.46% min^{-1}) (Table S1), with a residue yield of 69 wt% at 1000 °C.

The bio-type additives, SP, TA, SU and OP, present different thermal behavior compared to the coal and the synthetic polymers. A large quantity of volatiles is released before coal softening (<400 °C), during the pre-plastic stage (Table S1, Fig. 1). SP, SU and OP are less thermally stable than TA, and the generation of volatile compounds are between 76 and 82 wt% of the total decomposition products. Sawdust (SP) displays a thermogravimetric profile typical of lignocellulosic biomass (Fig. 3). The main DTG peak observed at 363 °C is assigned to the decomposition of cellulose and the shoulder at about 322 °C to hemicellulose, whereas the lignin decomposes slowly over a broad temperature interval, from 200 °C to above 500 °C [26]. Tannins (TA) are natural polyphenolic compounds, composed mostly of flavan-3-ol repeating units and smaller fractions of polysaccharides and sugars. TA presents a devolatilization in four stages: (i) <120 °C, which is attributed to the loss of moisture and absorbed gases, and represents only 3.7 wt%; (ii) 120–350 °C, where the primary decomposition takes place with a significant mass loss before 300 °C (21.8 wt%) and up to 400 °C of 34.4 wt%; (iii) 350–700 °C, where a small decomposition occurred with a weight loss of 10.3 wt% and the starting of charring reactions, and (iv) >700 °C, dominated by charring reactions with the release of small molecules. The complex condensed aromatic structure of tannin presents a high thermal resistance with a remaining weight at 1000 °C of about 27 wt%.

Sucrose (SU) undergoes caramelization during heating, which involves the formation of glucose and fructose anhydrides and their further condensation to polymeric products such as caramelan, caramelen and caramelin [31]. The residual mass is 24.5 and 16.1 wt%, at 500 and 1000 °C, respectively. The DTGmax also occurs below the fluid stage of the coal (Table S1, Fig. 3). The thermal decomposition takes place between 200 and 400 °C, with two maximum peaks of weight loss

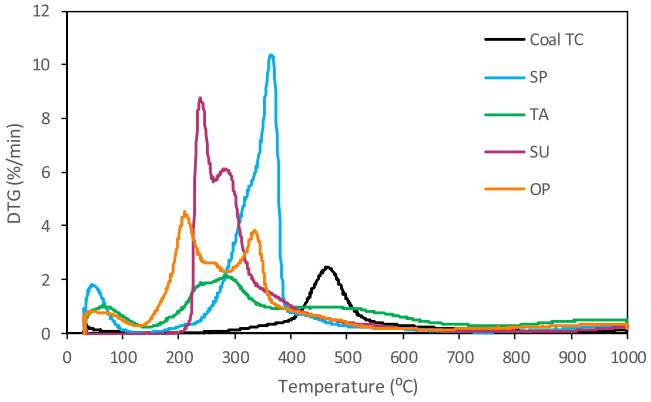

Fig. 3. Comparison of DTG curves of the bio-type additives and the coal.

at 234 and 282 °C (Fig. 3). For orange peel (OP) the DTG curve obtained shows a first stage below 120 °C, attributed to water desorption, followed by several stages partially overlapped in a large temperature range from 150 °C to 600 °C (Fig. 3). The volatile matter was produced up to 400 °C; it represents a 69 wt% and peaks at 209, 257 and 334 °C due to the decomposition of its components, pectin, hemicellulose and cellulose, respectively [32,33]. The mass loss above 400 °C can be attributed to lignin, which decomposes slowly over a very broad temperature range. The mass loss between 400 and 500 °C is only 6.5 wt%, so the interaction with the plastic stage of coal will be minimal. The residual mass at 1000 °C was 16.1 wt%.

Not only the bio-type additives show some different patterns in their thermal decomposition, but the morphology of the carbon products obtained at 500 °C are also different. Further thermogravimetric experiments were performed at a final temperature of 500 °C (the optimal temperature) to reveal the foaming capacity of the additives. The most remarkable findings are observed for PBP and SU. PBP leads to a residue with reticular carbon structure and fluid cell walls (Fig. S1), similar to that obtained in foams derived from thermosetting materials such as phenolic resins [1], and SU is the bio-type additive that shows swelling capacity with an appearance of sponge (Fig. S1), which is consistent with its foaming capacity [34].

3.3. Interactions between coal and additives

In the first stage of the preparation of carbon foams, the comparison of the individual thermal behavior of the blend components gives some guides in relation to the potential interaction of the precursors. To acquire additional and useful data for identifying potential combination effects between the coal and each additive, the thermogravimetric analysis of the blends with increasing amounts of the additive up to 50 wt% were also evaluated. The blends of coal and each organic additive can give different kinds of interactions (synergy, antagonism and non-interactive) and they can occur over a broad range of concentrations; i.e., various ratios should be tested.

The profiles of the DTG curves obtained for the blends are very similar for a given type of additives (synthetic polymers and bio-additives); then, only one representative blend of each group will be commented in detail: TC+LDPE and TC+SP (Figs. 4a and 5a, respectively). The remaining blends are included in the Supplementary Information (Figs. S2-S6).

The thermal decomposition of LDPE overlaps with that of coal giving a single DTG peak in a temperature interval ranging from 400 to 500 °C (Fig. 4a). By applying the additivity law, no synergetic effect during co-pyrolysis can be observed in terms of the carbonaceous solid produced at 500 °C (Fig. 4b), suggesting an independent VM evolution. No evidence of synergy effect was observed for PET and PBP either (Figs. S2-S3). Thus, the increase in the fluidity measured in TC+ 5PBP and TC+ 10PBP blends should be attributed to the fluidity of the polymer, not to a real chemical interaction between the coal and the additive. For blends TC+SP, however, two devolatilization steps occur (Fig. 5a). The low-temperature peaks in the DTG curve (<400 °C) correspond to the bio-additive, whereas the peak at around 467 °C corresponds to the VM release from coal. As the percentage of bio-additive in the blend increases, so do their decomposition peaks and the coal released decreases in a similar trend. These results together with the correlation obtained between experimental and calculated carbonaceous solid yields (Fig. 5b) indicate that no interactions take place during co-pyrolysis. The absence of synergetic effect was also found for TA, SU and OP (Figs. S4-S6).

3.4. Carbon foams prepared from the binary blends

Considering the results obtained so far, it is noticed that: (i) the volatiles derived from the additives evolve without any chemical participation in the solvolysis process under the experimental conditions of TG analysis; and (ii) the Gieseler plastometry demonstrates the existence of physical interactions between the blend components that decrease the fluidity of the coal and shorten, in some cases, the temperature plastic range, as shown in Table 2. PET and sucrose do not seem to be suitable additives for carbon foam synthesis, since, depending on its concentration, they cause a great loss or the near total loss of coal fluidity. Consequently, PET is discarded as a carbon foam precursor. Sucrose, however, is known as an excellent foam precursor, since during heating at ambient pressure it becomes fluid and swells [34–36], as it is clearly evidenced by the appearance of the char derived from TGA experiments at 500 °C (Fig. S1). For the rest of additives, which act reducing fluidity, it should be also taken into account that coal-based carbon foams can also be prepared from low-fluidity coals (<20 ddpm) [13,21]. Therefore, if the additive modifies the fluidity parameters within the range of optimum values to allow foaming, it should be possible to obtain suitable carbon foams derived from blends with coal. Moreover, in a pressurized reactor, the volatile matter is retained in the reaction media, and changes in the composition of the gases produced (such as the presence of oxygenated-compounds or more hydrogen) may modify the degree of fluidity. Thus, considering that the results obtained by Gieseler plastometry and TG analysis give preliminary but not conclusive information for foam synthesis, the next step is to find the optimal conditions for chemical and physical interactions to obtain a carbonaceous porous structure with a suitable cross-linked matrix and an adequate distribution of pores. In this context, foams derived from blends containing 10 wt% of each additive under pressurized conditions were synthetized. Larger amounts (20 wt%) were also employed for OP

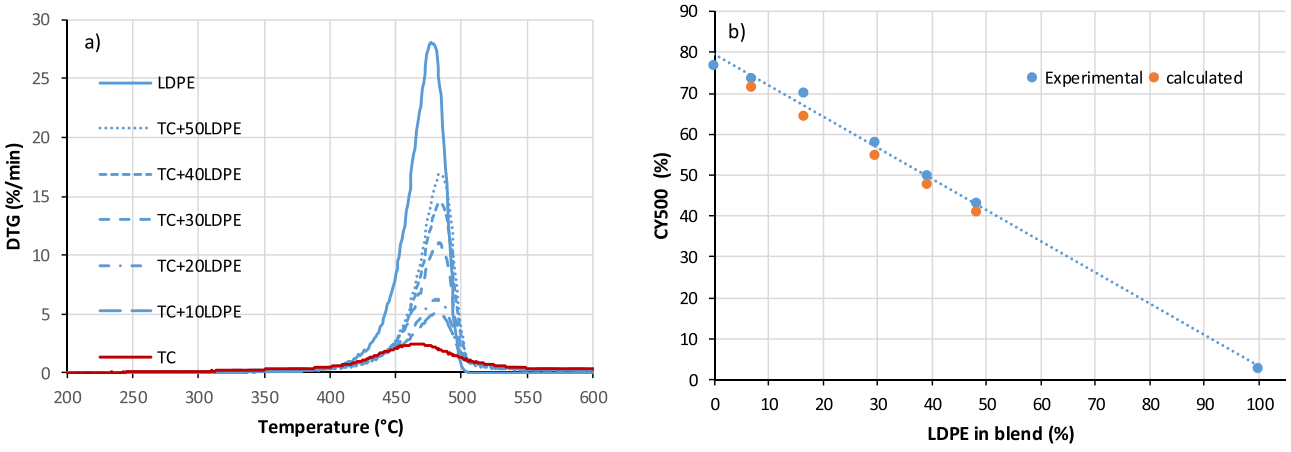

Fig. 4. DTG curves corresponding to the blends of coal TC and LDPE (a), and relationship between the percentage of LDPE in the blend and the experimental and calculated char yield at 500 °C (b).

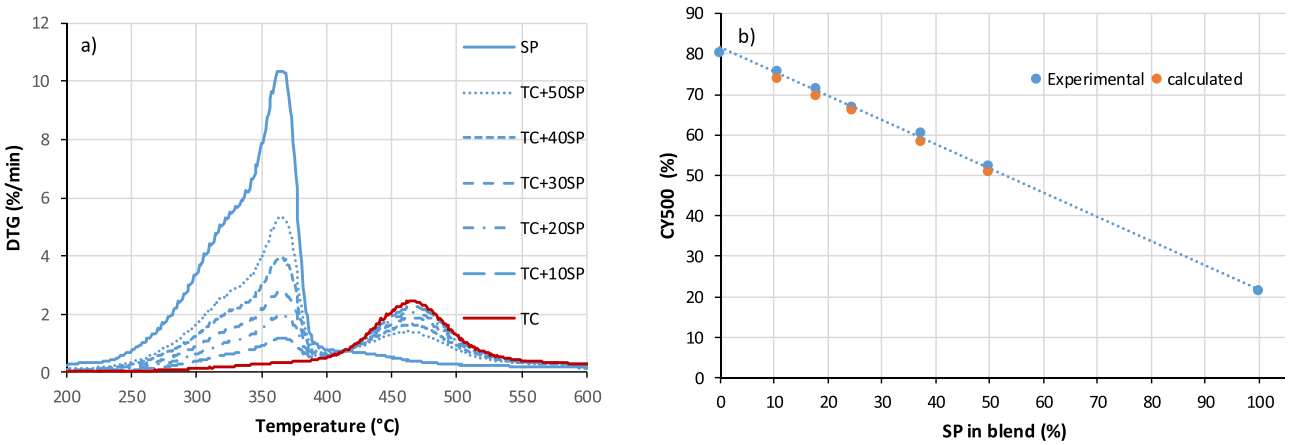

Fig. 5. DTG curves corresponding to the blends of coal TC and SP (a), and relationship between the percentage of SP in the blend and the experimental and calculated char yield at 500 °C (b).

and SU, while the amount of LDPE was limited at a 5 wt%.

SEM assessment allowed the detailed analysis of the morphology of the carbon foam surface. All the carbon foams consist of a network made of cells with an average size of 1 mm. The cells are connected by the presence of pores in the carbon walls with a size of around 100 μm (Fig. 6a). The micrographs presented in Figs. 6 and 7 confirm that the incorporation of additives to the raw coal do not prevent the development of the cellular structure of the foams. For blends with bio-type additives, SEM images show a homogenous structure with primary cells of lower dimensions (Fig. 7). However, for synthetic polymer LDPE and rubber PBP, the corresponding foams display heterogeneous structure with larger cells for CF5LDPE and less porosity in the walls of the cells for CF10PBP (Fig. 6b and c).

The apparent density of coal-based carbon foams is closely related with the fluidity and the pressure generated during the foaming step. Thus, the apparent density of the foam decreases with the increasing fluidity of precursor coal [13,14,21]. However, the results of this study reveal that the use of bio-additives gives rise to foams of lower apparent density values and higher total pore volumes than the foam derived from the individual coal, despite their lower fluidity (Table 3). On the contrary, the synthetic polymers, PBP and LDPE, lead to high density foams.

To explain the better development of porosity with the addition of bio-type additives, several parameters should be considered other than fluidity, such as the volatiles released and the pressure generated inside the reactor. Unlike in Gieseler plastometry, the volatiles generated during foaming remain in the reactor, so these species can act as "solvating" agents. Specifically, oxygen- and hydrogen-rich species cause changes in fluidity during foaming and render carbon foams of lower density. As it was pointed out by TG experiments, blends derived from coal/bio-type additives release a large quantity of these products before coal-softening. Most of the degradation products correspond to highly reactive oxygenated compounds that may interact with the free radicals derived from the cracking reactions of the coal, improving fluidity under pressurized conditions, promoting cross-linking reactions and resulting in a better porosity development. As it can be observed in Table 3, the additives SP, SU and TA render foams with higher H/C content. The texture of the resulting foam is also related to the pressure generated inside the reactor [15,28]. When foams are prepared from coal/OP and coal/SU blends, the final pressure gradually increases from the 66 bar reached with the coal to 75 and 100 bar obtained for CF10OP/CF10SU and CF20OP/CF20SU, respectively. The increased foaming pressure under the same temperature may produce an increase in the fluidity of the coal, since the release of the volatile matter from coal is hampered, remaining in the coal matrix and causing a decrease of the viscosity with respect to the values reported by the Gieseler test [28]. Therefore, foams of higher pore volume were obtained (Table 3).

On the opposite side, addition of LDPE and PBP renders carbon foams of higher apparent density. Furthermore, the helium picnometry analysis performed over these samples in pieces and powder shape, reveals the existence of close porosity in such foams, since the values where higher in the powdered samples (Table 3). Despite volatile release in the plastic stage of the carbons no interactions were observed in TGA experiments. Therefore, it is expected that the high pressure generated during the plastic stage of the coal promotes condensation reactions, hindering the foaming process and rendering high-density foams due to a blocking of some pores in the C-foams by the deposition of the molten LDPE and/or oligomers from thermal decomposition.

According to the data detailed in Table 3, the order from more to less porosity is as follows:

TC10SP > TC5SP > TC20OP > TC10OP > TC10TA > TC20SU > TC10SU ≈TC > TC20PBP > TC5LDPE

These findings suggest that a better porosity development can be achieved by the use of bio-type additives, while synthetic polymers, such as thermoplastics and elastomers, seem unsuitable additives for the production of carbon foams derived from coal.

The pore size distribution obtained by mercury porosimetry is presented in Fig. 8. It can be clearly observed that CF has a higher volume of mercury intrusion compared to CF5LDPE (Fig. 8a). However, the pore size range is not affected by the presence of the additive, according to the similar curves obtained. Both samples present a mean pore size of around 110 μm. By contrast, sample CF10PBP shows a wider pore size distribution with a smaller mean pore size, around 70 μm. Fig. 8b compares the pore size distributions of carbon foams derived from the blends with 10 wt% of bio-type additives. It can be observed that all the samples present porosity sizes of 170–20 μm, with a more substantial presence of pores of lower size compared to CF, which ranges between 90 and 50 μm. The effect is more marked for CF10SP, whose mean pore size shifts from 110 μm for CF to 80 μm. However, CF10SU has a mean pore size slightly higher, around 130 μm. The rise to 20 wt% of the additive amount for OP and SU gives rise to an increase in the proportion of pores with sizes between 90 and 20 μm (Fig. 8b).

3.4.1. *Effect of additives on thermal conductivity*

Specific heat, thermal diffusivity and thermal conductivity data of carbon foams with different additives at 10 wt% are reported in Table 4. CF5LDPE is not included is this study, since it was not possible to obtain a piece with the necessary dimensions for the experimental tests, due to its cell network.

The thermal conductivity of the coal-based carbon foam (CF) is around 3 W m^{-1} K^{-1}. However, when additives are incorporated to the coal, a decrease in the values can be observed for all the resultant foams,

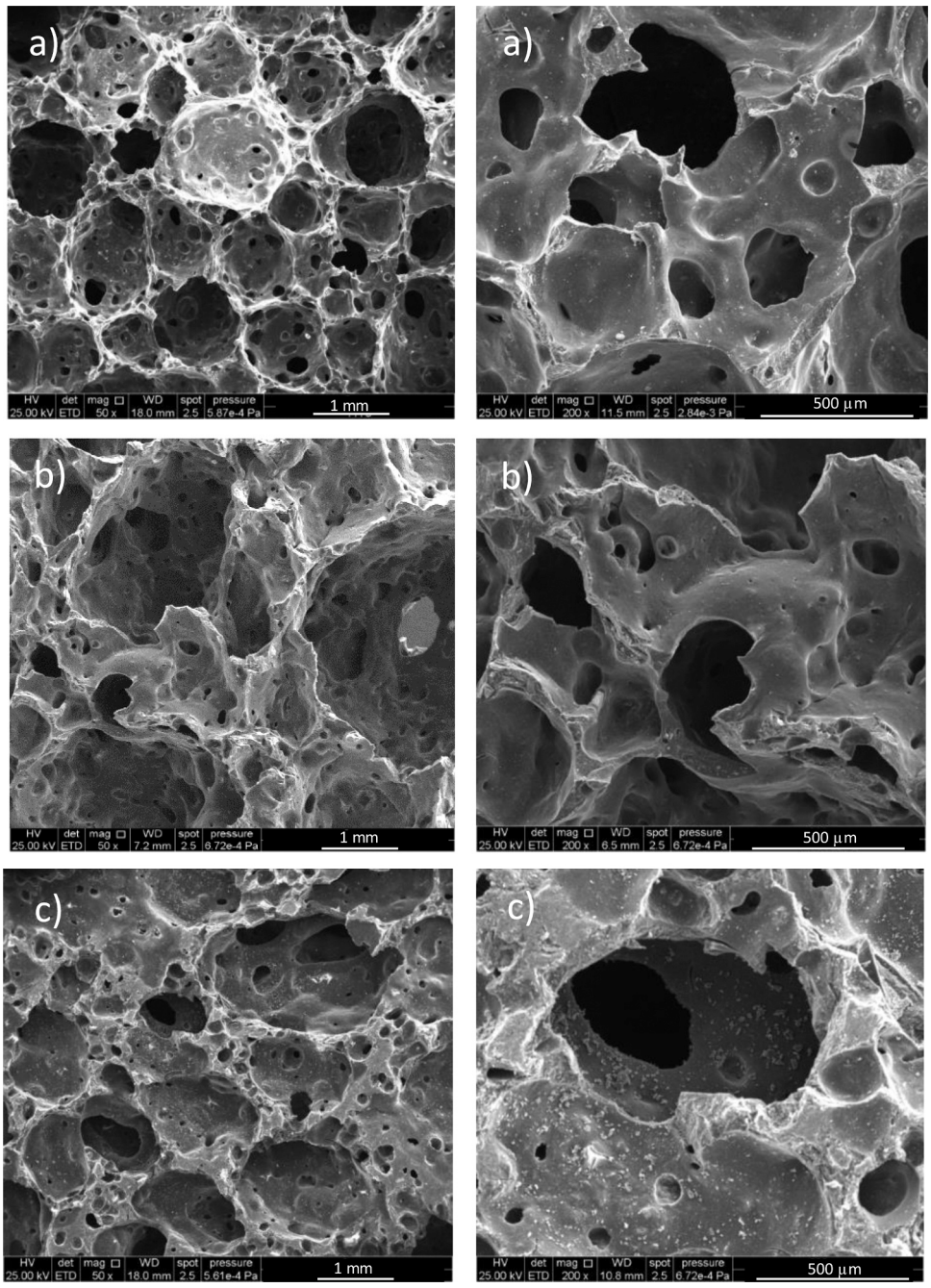

Fig. 6. SEM micrographs of several carbon foams: (a) carbon foam from coal TC (displayed as a reference), (b) CF5LDPE, and (c) CF10PBP.

ranging from 1.5 to 0.7 W m^{-1} K^{-1}. SU and PBP display similar values (1.5 W m^{-1} K^{-1}), whereas those derived from SP, OP and TA show values lower than 1 W m^{-1} K^{-1}. The values of thermal conductivity are within the range to those reported for commercial CFoam®, which can be employed as thermal insulator and in seasonal storage applications based on phase-change materials [10,37,38].

Thermal conductivity is a property related to the pore structure (density, cell size) and the carbon structure (the degree of graphitization and the presence of heteroatoms) [5,39]. The different nature and composition of the additives used in this study does not allow establishing a correlation between thermal conductivity and bulk density. However, the results can be interpreted by the additive nature. Thus, the heterogeneous structure and closed porosity showed by TC10PBP can make heat transmission difficult, decreasing thermal conductivity compared to the reference TC foam [17]. In the case of bio-type additives, the porosity follows an opposite trend, in such manner that the apparent density decreases. A relation with the D/G Raman parameter confirms that the incorporation of SP, SU, OP and TA leads to a more disordered carbon foams (Fig. 9), which is consistent with their non-graphitizable nature and a complex mechanism involving cross-linking during the foaming process. Therefore, the lower thermal conductivity values can be attributed in these foams to the fact that bio-type additives limit the stacking of aromatic layers, hindering the conduction of heat.

4. Conclusions

Biomass, biomolecules and polymers founded in wastes from agriculture, automotive and urban origin can be used as additives for coal-based carbon foam synthesis. Cellular carbon foams were successfully

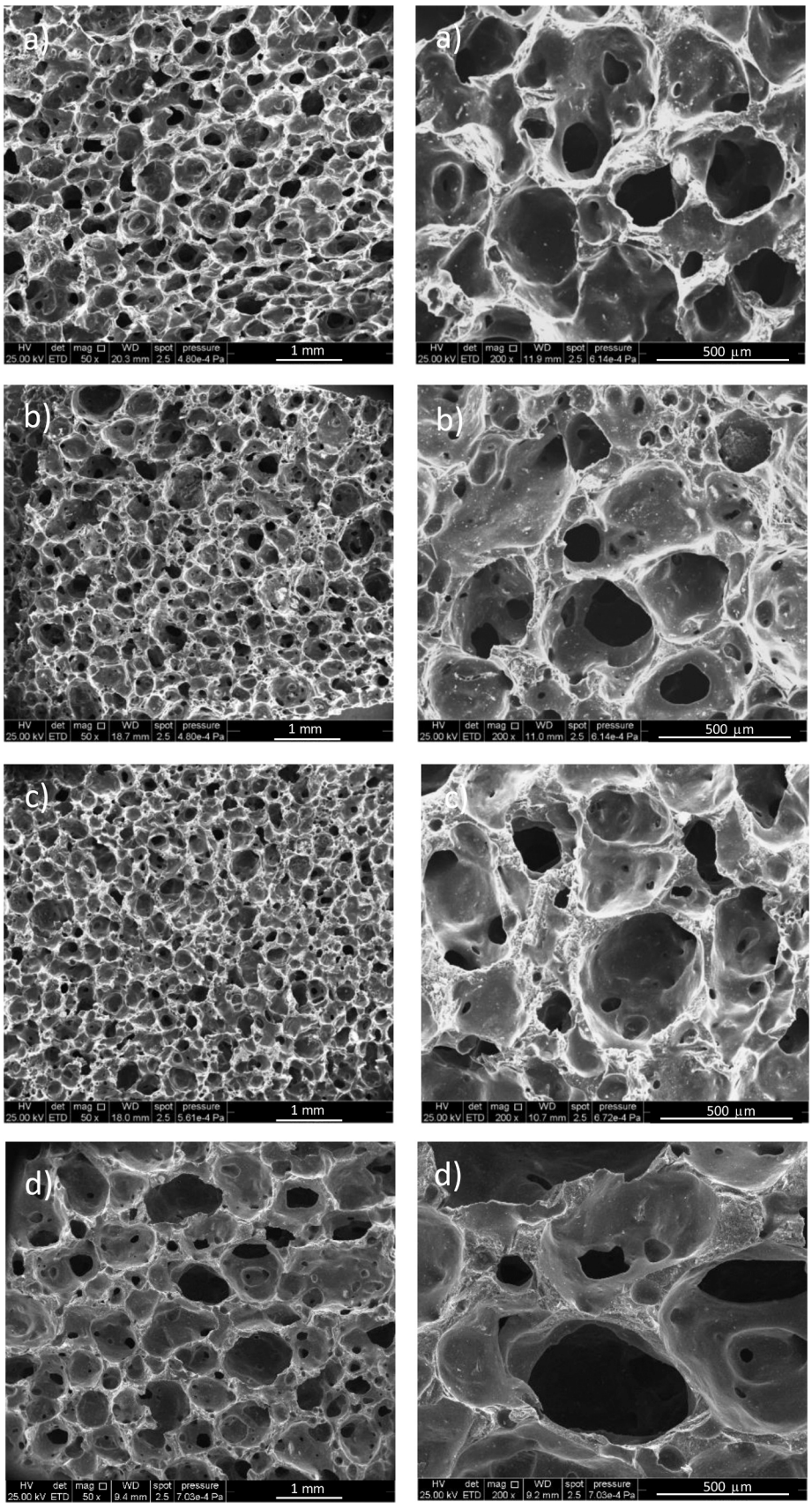

Fig. 7. SEM micrographs of several carbon foams: (a) CF10SP, (b) CF10TA, (c) CF10SU and (d) CF10OP.

Table 3
Structural properties of the carbon foams derived from the coal and the binary blends.

	Additive (%)	Pr (bar)	ρ_{He} (g cm^{-3})	ρ_{Hg} (g cm^{-3})	Ɛ (%)	V_{tp} (cm^3 g^{-1})	H/C	O/C
CF	0	66	1.89	1.01	46.6	0.46	0.0238	0.0024
CF5LDPE	5	15*	1.76/1.87**	1.14	35.1/39.0	0.31	0.0145	0.0009
CF10PBP	10	86	1.76/1.86**	1.07	39.2/42.6	0.40	0.0182	0.0019
CF5SP	5	46	2.21	0.67	69.6	1.04	0.0339	0.0010
CF10SP	10	23	1.92	0.58	69.8	1.20	0.0408	0.0015
CF10TA	10	50	1.78	0.77	56.6	0.74	0.0385	0.0033
CF10SU	10	75	1.84	0.97	47.3	0.49	0.0285	0.0017
CF20SU	20	95	1.72	0.88	48.8	0.55	0.0337	0.0018
CF10OP	10	75	1.97	0.70	58.6	0.76	0.0168	0.0030
CF20OP	20	100	1.86	0.77	64.5	0.92	0.0205	0.0029

* Clogged tube; * * Data obtained in piece/powder
Pr: final foaming pressure; ρ_{He}: helium true density; ρ_{Hg}: apparent density; Ɛ: open porosity; V_{tp}: total pore volume

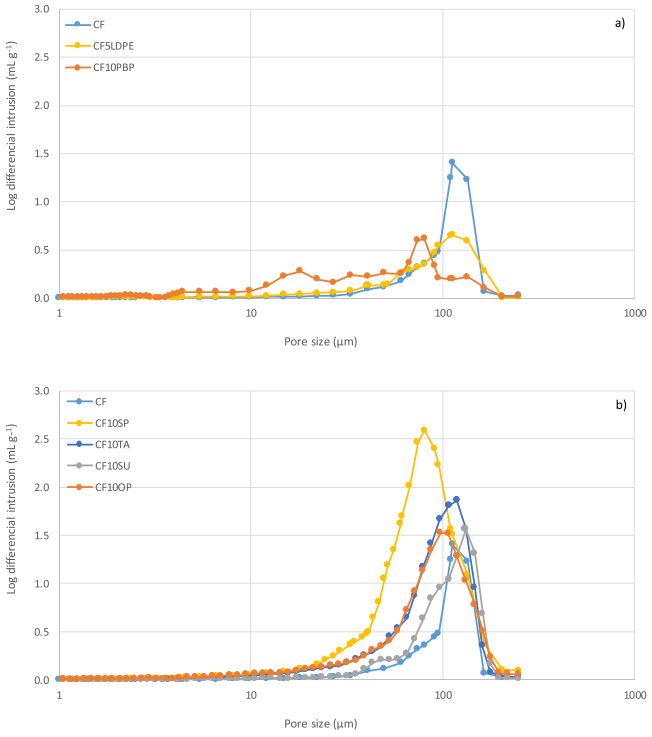

Fig. 8. Pore size distribution obtained by mercury porosimetry: (a) carbon foams CF, CF5LDPE and CF10PBP, and (b) carbon foams CF, CF10SP, CF10TA, CF10SU and CF10OP.

Table 4
Thermal parameters measured at 25 °C.

Sample	C_P (J g^{-1} K^{-1})	α (mm^2 s^{-1})	*k* (W m^{-1} K^{-1})
CF	0.80	3.40	2.75
CF10PBP	0.76	1.74	1.41
CF10SP	0.71	2.11	0.87
CF10TA	0.72	2.67	0.74
CF10SU	0.72	3.20	1.47
CF10OP	0.67	1.96	0.92

Cp: specific heat; α: thermal diffusivity; *k*: thermal conductivity

synthesized, using blends in which a bituminous coal was selected as the main precursor. The foaming mechanism of the blends and the properties of the resultant foams showed that bio-type additives (orange peel, pine sawdust, tannins and sucrose) had a beneficial impact on porosity development, whereas synthetic polymers (polyolefins and elastomers) had the opposite effect.

The interaction of coal and additives evaluated by the Gieseler test

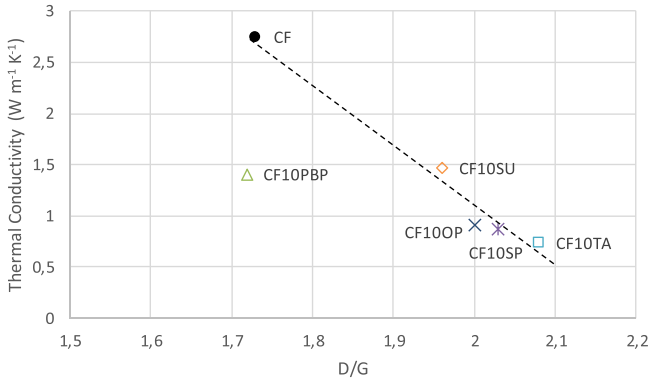

Fig. 9. Thermal conductivity as a function of Raman parameter D/G.

showed that the incorporation of additives to coal produced a reduction in the plastic properties of the blends, except for the elastomer PBP. During the co-pyrolysis of the binary blends by using thermogravimetry, the volatiles evolved independently without any synergetic effect for all the additives evaluated. The generation of volatile products in the case of synthetic polymers (LDPE, PET and PBP) overlaps with the starting of VM evolution of coal. The pressure generated inside the reactor during the plastic stage of the coal may promote condensation reactions, rendering foams of higher density. In addition, the low fluidity showed by the blend with PET impeded the foam synthesis.

Bio-type additives release the highest amount of volatiles at low temperature (<400 °C), so the reduction in the thermoplastic properties of blends can be a consequence of the oxygen-rich species evolving before the softening of coal. During foaming in a pressurized reactor, an opposite effect may occur. In that case, the volatiles released before the plastic stage can interact among themselves and with the free radicals derived from the cracking reactions of the coal. In addition, a higher pressure in the initial foaming stages may also increase fluidity. As a consequence, the use of bio-type additives renders foams of lower density, higher porosity and worse thermal properties than those of its counterpart derived from the unblended coal. A relationship between thermal conductivity and the disorder degree of the carbon matrix derived by microRaman spectroscopy was established.

CRediT authorship contribution statement

All persons who meet authorship criteria are listed as authors, and the corresponding author certifies that all the authors have participated sufficiently in the work to take public responsibility for the content, including participation in the concept, design, analysis, writing, or revision of the manuscript. Furthermore, the corresponding author certifies that this material or similar material has not been and will not be submitted to or published in any other publication before its

appearance in the Journal of Analytical and Applied Pyrolysis.

Declaration of Competing Interest

The authors declare that they have no known competing financial interests or personal relationships that could have appeared to influence the work reported in this paper.

Acknowledgments

This work was supported by PCTI Asturias (research project GRUPIN ID2018–000234).

Appendix A. Supporting information

Supplementary data associated with this article can be found in the online version at doi:10.1016/j.jaap.2021.105359.

References

[1] B. Nagel, S. Pusz, B. Trzebicka, Review: tailoring the properties of macroporous carbon foams, J. Mater. Sci. 49 (2014) 1–17, https://doi.org/10.1007/s10853-013-7678-x.
[2] H. Liu, S. Wu, N. Tian, F. Yan, C. You, Y. Yang, Carbon foams: 3D porous carbon materials holding immense potential, J. Mater. Chem. A 8 (2020) 23699–23723, https://doi.org/10.1039/d0ta08749a.
[3] E. Stojanovska, M.D. Calisir, N.D. Ozturk, A. Kilic, Carbon-based foams: preparation and applications, in: Nanocarbon Its Compos. Prep. Prop. Appl., Elsevier, 2018, pp. 43–90, https://doi.org/10.1016/B978-0-08-102509-3.00003-1.
[4] M. Inagaki, J. Qiu, Q. Guo, Carbon foam: preparation and application, Carbon 87 (2015) 128–152, https://doi.org/10.1016/j.carbon.2015.02.021.
[5] P. Jana, V. Fierro, A. Pizzi, A. Celzard, Biomass-derived, thermally conducting, carbon foams for seasonal thermal storage, Biomass Bioenergy 67 (2014) 312–318, https://doi.org/10.1016/j.biombioe.2014.04.031.
[6] M. Vinícius, G. Zimmermann, D. Perondi, Lídia, K. Lazzari, M. Godinho, J. Ademir, Zattera, Carbon foam production by biomass pyrolysis, J. Porous Mater. 27 (2020) 1119–1125, https://doi.org/10.1007/s10934-020-00888-y.
[7] O. Smorygo, A. Marukovich, V. Mikutski, V. Stathopoulos, S. Hryhoryeu, V. Sadykov, Tailoring properties of reticulated vitreous carbon foams with tunable density, Front. Mater. Sci. 10 (2016) 157–167, https://doi.org/10.1007/s11706-016-0338-8.
[8] S. Beluns, S. Gaidukovs, O. Platnieks, G. Gaidukova, I. Mierina, L. Grase, O. Starkova, P. Brazdausks, V.K. Thakur, From wood and hemp biomass wastes to sustainable nanocellulose foams, Ind. Crops Prod. 170 (2021), 113780, https://doi.org/10.1016/J.INDCROP.2021.113780.
[9] A.B.R. Loison, P. Foch, Coke — Quality and production, Butterworth-Heinemann, London, 1989, https://doi.org/10.1016/0008-6223(89)90053-5.
[10] N.C. Gallego, J.W. Klett, Carbon foams for thermal management, Carbon 41 (2003) 1461–1466, https://doi.org/10.1016/S0008-6223(03)00091-5.
[11] J. Klett, R. Hardy, E. Romine, C. Walls, T. Burchell, High-thermal-conductivity, mesophase-pitch-derived carbon foams: effect of precursor on structure and properties, Carbon 38 (2000) 953–973, https://doi.org/10.1016/S0008-6223(99)00190-6.
[12] J.W. Klett, A.D. McMillan, N.C. Gallego, T.D. Burchell, C.A. Walls, Effects of heat treatment conditions on the thermal properties of mesophase pitch-derived graphitic foams, Carbon 42 (2004) 1849–1852, https://doi.org/10.1016/j.carbon.2004.01.057.
[13] M. Grujicic, C.L. Zhao, S.B. Biggers, D.R. Morgan, Experimental investigation and modeling of effective thermal conductivity and its temperature dependence in a carbon-based foam, 2006 418, J. Mater. Sci. 41 (2006) 2309–2317, https://doi.org/10.1007/S10853-006-7169-4.
[14] CFOAM® Carbon Foam - CFOAM® Carbon Foam, (n.d.). ⟨https://www.cfoam.com/whatis/⟩ (Accessed July 5, 2021).
[15] M. Calvo, R. García, S.R. Moinelo, Carbon foams from different coals, Energy Fuels 22 (2008) 3376–3383, https://doi.org/10.1021/ef8000778.
[16] C. Chen, E.B. Kennel, A.H. Stiller, P.G. Stansberry, J.W. Zondlo, Carbon foam derived from various precursors, Carbon 44 (2006) 1535–1543, https://doi.org/10.1016/j.carbon.2005.12.021.
[17] X. Wang, J. Zhong, Y. Wang, M. Yu, A study of the properties of carbon foam reinforced by clay, Carbon 44 (2006) 1560–1564, https://doi.org/10.1016/j.carbon.2005.12.025.
[18] W.Q. Li, H.B. Zhang, X. Xiong, F. Xiao, A study of the properties of mesophase-pitch-based foam/graphitized carbon black composites, Mater. Sci. Eng. A 528 (2011) 2999–3002, https://doi.org/10.1016/j.msea.2010.12.013.
[19] J. Yang, Z.-M. Shen, R.-S. Xue, Z.-B. Hao, Study of mesophase pitch-based graphite foam used as anodic materials in lithium ion rechargeable batteries, 2005 405. J. Mater. Sci. 40 (2005) 1285–1287, https://doi.org/10.1007/S10853-005-6953-X.
[20] J. Rodríguez-García, I. Cameán, A. Ramos, E. Rodríguez, A.B. García, Graphitic carbon foams as anodes for sodium-ion batteries in glyme-based electrolytes, Electrochim. Acta 270 (2018) 236–244, https://doi.org/10.1016/j.electacta.2018.03.084.
[21] E. Rodríguez, I. Cameán, R. García, A.B. García, Graphitized boron-doped carbon foams: performance as anodes in lithium-ion batteries, Electrochim. Acta 56 (2011) 5090–5094, https://doi.org/10.1016/j.electacta.2011.03.078.
[22] E. Rodríguez, R. García, Characterisation of boron-doped coal-derived carbon foams and their oxidation behaviour, Fuel 93 (2012) 288–297, https://doi.org/10.1016/j.fuel.2011.08.028.
[23] E. Rodríguez, R. García, Microporosity development in coal-based carbon foams, Energy Fuels 26 (2012) 3703–3710, https://doi.org/10.1021/ef300193c.
[24] E. Rodríguez, R. García, Low-cost hierarchical micro/macroporous carbon foams as efficient sorbents for CO 2 capture, Fuel Process. Technol. 156 (2017) 235–245, https://doi.org/10.1016/j.fuproc.2016.09.002.
[25] M.A. Diez, A.G. Borrego, Evaluation of CO_2-reactivity patterns in cokes from coal and woody biomass blends, Fuel 113 (2013) 59–68, https://doi.org/10.1016/j.fuel.2013.05.056.
[26] M.A. Diez, R. Alvarez, M. Fernández, Biomass derived products as modifiers of the rheological properties of coking coals, Fuel 96 (2012) 306–313, https://doi.org/10.1016/j.fuel.2011.12.065.
[27] M.A. Diez, R. Alvarez, S. Melendi, C. Barriocanal, Feedstock recycling of plastic wastes/oil mixtures in cokemaking, Fuel 88 (2009) 1937–1944, https://doi.org/10.1016/j.fuel.2009.03.035.
[28] M. Calvo, R. García, A. Arenillas, I. Suárez, S.R. Moinelo, Carbon foams from coals. A preliminary study, Fuel 84 (2005) 2184–2189, https://doi.org/10.1016/j.fuel.2005.06.008.
[29] A. Cuesta, P. Dhamelincourt, J. Laureyns, A. Martínez-Alonso, J.M.D. Tascón, Raman microprobe studies on carbon materials, Carbon 32 (1994) 1523–1532, https://doi.org/10.1016/0008-6223(94)90148-1.
[30] M.A. Díez, C. Barriocanal, R. Álvarez, Plastic wastes as modifiers of the thermoplasticity of coal, Energy Fuels 19 (2005) 2304–2316, https://doi.org/10.1021/ef0501041.
[31] P. Jana, V. Fierro, A. Celzard, Sucrose-based carbon foams with enhanced thermal conductivity, Ind. Crops Prod. 89 (2016) 498–506, https://doi.org/10.1016/j.indcrop.2016.06.001.
[32] R. Miranda, D. Bustos-Martinez, C.S. Blanco, M.H.G. Villarreal, M.E.R. Cantú, Pyrolysis of sweet orange (Citrus sinensis) dry peel, J. Anal. Appl. Pyrolysis. 86 (2009) 245–251, https://doi.org/10.1016/j.jaap.2009.06.001.
[33] B. Zapata, J. Balmaseda, E. Fregoso-Israel, E. Torres-García, Thermo-kinetics study of orange peel in air, 2009 981. J. Therm. Anal. Calorim. 98 (2009) 309–315, https://doi.org/10.1007/S10973-009-0146-9.
[34] M.J.G. De Araújo, J. Villarroel-Rocha, V.C. De Souza, K. Sapag, S.B.C. Pergher, Carbon foams from sucrose employing different metallic nitrates as blowing agents: application in CO_2 capture, J. Anal. Appl. Pyrolysis. 141 (2019), 104627, https://doi.org/10.1016/J.JAAP.2019.05.016.
[35] R. Narasimman, K. Prabhakaran, Preparation of low density carbon foams by foaming molten sucrose using an aluminium nitrate blowing agent, Carbon 50 (2012) 1999–2009, https://doi.org/10.1016/j.carbon.2011.12.058.
[36] Y. Shi, G. Liu, L. Wang, H. Zhang, Heteroatom-doped porous carbons from sucrose and phytic acid for adsorptive desulfurization and sulfamethoxazole removal: a comparison between aqueous and non-aqueous adsorption, J. Colloid Interface Sci. 557 (2019) 336–348, https://doi.org/10.1016/J.JCIS.2019.09.032.
[37] V. Canseco, Y. Anguy, J.J. Roa, E. Palomo, Structural and mechanical characterization of graphite foam/phase change material composites, Carbon 74 (2014) 266–281, https://doi.org/10.1016/J.CARBON.2014.03.031.
[38] Spec Sheets - CFOAM® Carbon Foam, (n.d.). ⟨https://www.cfoam.com/spec-sheets/⟩ (Accessed July 15, 2021).
[39] R. Kumar, H. Jain, A. Chaudhary, S. Kumari, D.P. Mondal, A.K. Srivastava, Thermal conductivity and fire-retardant response in graphite foam made from coal tar pitch derived semi coke, Compos. Part B Eng. 172 (2019) 121–130, https://doi.org/10.1016/J.COMPOSITESB.2019.05.036.